A sulfonated covalent organic framework for atmospheric water harvesting

Paul Schweng,[a,c] Changxia Li,[b] Patrick Guggenberger,[b,c] Freddy Kleitz,[b]* Robert T. Woodward[a]*

[a] Institute of Materials Chemistry and Research, Faculty of Chemistry, University of Vienna, Währinger Straße 42, 1090, Vienna, Austria

[b] Department of Functional Materials and Catalysis, Faculty of Chemistry, University of Vienna, Währinger Straße 42, 1090 Vienna, Austria

[c] Vienna Doctoral School in Chemistry, University of Vienna, Währinger Straße 42, 1090, Vienna, Austria

Keywords: Atmospheric water harvesting; covalent-organic frameworks; porous organic materials; separation; adsorption; direct air capture

Abstract

We report a sulfonated covalent organic framework (COF) capable of atmospheric water harvesting in arid conditions. The isothermal water uptake profile of the framework was studied, and the network displayed steep water sorption at low relative humidity (RH) in temperatures of up to 45 °C, reaching a water uptake of 0.12 $g \cdot g^{-1}$ at 10% RH and even 0.08 $g \cdot g^{-1}$ at just 5% RH, representing some of the most extreme conditions on the planet. We found that the inclusion of sulfonate moieties shifted uptake in the water isotherm profiles to lower RH compared to non-sulfonated equivalents, demonstrating well the benefits of including these hydrophilic sites for water uptake in hot arid locations. Repeated uptake and desorption were performed on the network without significant detriment to its adsorption performance, demonstrating the potential of the sulfonated COF for real-world implementation.

Introduction

The United Nations estimates that today one-third of the world`s population does not have access to safely managed drinking water and sanitation services. To address this, the United Nations' Sustainable Development Goal (UN SDG) #6 set a target for providing sanitation and clean water to all by the year 2030.[1] To be able to achieve UN SDG #6 within this timeframe, substantial improvements in current water harvesting and purification methods are required. Seawater desalination is a promising approach for freshwater production, however, it is somewhat limited by the energy intensity of the process and, perhaps more crucially, the need for access to bodies of salty water render it unsuitable for dry landlocked regions.[2,3]

In search of a broader solution, atmospheric water harvesting (AWH) has emerged as an alternative capable of providing a supplementary, geographically unrestricted source of fresh water.[4] The water in air is estimated to be 1.3×10^{16} L, far exceeding the volume of fresh water in all of the world's rivers (2.1×10^{15} L).[5] AWH exploits atmospheric water by using sorbent materials to passively capture water from air and concentrate it at their surface. Upon the application of some trigger, such as heat, the water is then desorbed from the sorbent in a controlled manner for harvesting. Ideal sorbents for AWH should display long-term stability upon exposure to water and heat, good working capacities below 30% relative humidity (RH), and heat of adsorption favourable to low-energy water desorption.[6]

Zeolites[7] and hygroscopic metal salts[8] display good water-sorption capacities, but typically suffer from high adsorption enthalpies, rendering water release energetically demanding. Metal-organic frameworks (MOFs) have shown promise for AWH due to their high uptake capacities and low enthalpies of adsorption.[9] Owing to their desirable properties and good performance, some MOFs have recently been applied practically in large-scale devices.[10] However, the vast majority of MOFs are unstable upon exposure to water, leading to network degradation. Furthermore, more water-stable MOFs could still pose health risks due to the potential leakage of metals into the harvested water.[11] Hence, research on new sorbents for

AWH has recently focused on porous organic materials, such as covalent organic frameworks (COFs).[12]

Covalent organic frameworks are a class of reticular materials that are synthesised from molecular organic building blocks linked together using reversible condensation reactions.[13] COFs exhibit a range of advantageous features, including high crystallinity, permanent porosity, and a large specific surface area. The wealth of viable structural building blocks and linkages offer some degree of control over the chemical and textural properties, enabling bottom-up application-targeted design.[14] However, successful water sorption in COFs often requires high RH for uptake and large energy input for regeneration due to hysteresis upon water desorption.[15] In an attempt to improve their water uptake, various functional groups were incorporated into the chemical structure of the building blocks of ketoenamine-linked COFs.[16] The incorporation of hydrophilic nitro or hydroxy groups into the backbone led to a shift in the onset of water adsorption to lower RH and improved overall performance. Elsewhere, improvements in hydrophilicity in isostructural azine-linked COFs were achieved by introducing hydroxy groups, again shifting uptake onset to lower RH.[17] Similarly, the replacement of phenyl groups with pyridine units in a COF backbone shifted the onset of significant water uptake from 65% to 25% RH, while retaining the absolute capacity.[18] Aside from modifications of COF surface chemistry, pore size has also been identified as a crucial factor for the water uptake performance.[12] To support water condensation, pore diameters should ideally be between 0.8 and 2 nm, as demonstrated for an imine-linked COF with a voided square grid[19] and a hydrophobic trigonal COF.[20] In contrast to the bottom-up design of COFs via careful choice of their organic building blocks, post-synthetic strategies have emerged as a supplementary route to improved water uptake at lower RH. For example, the post-synthetic oxidation of hydrazine to the hydrazide-linked COFs resulted in a shift in the onset of water adsorption to lower RH without impacting the total uptake capacity.[21] More recently, a post-synthetic strategy was employed to produce nitrone-linked COFs with improved water uptake at low RH from imine- and amine-linkages, however, with the detrimental effect of reducing the overall capacity from 0.34 to 0.27 $g \cdot g^{-1}$.[15] Despite the ongoing research into improved adsorbents for AWH, the

number of COFs with suitable water uptake at 30% RH remains limited and many of these networks cannot capture water below 20% RH,[22,23,24] representing some of the harshest environments on Earth.

Recently, we reported a sulfonated hypercrosslinked polymer (SHCP-10) able to adsorb significant amounts of water from air even at <10% RH.[25] We demonstrated that highly hygroscopic sulfonate groups are excellent candidates for enhancing the water sorption performance of hydrophobic carbonaceous materials, as our non-sulfonated reference exhibited negligible water uptake <70% RH. Here, we adapted this concept in a COF to exploit its crystalline nature and narrow pore size distribution. We describe a sulfonate-decorated COF possessing a steep uptake in the water sorption isotherm at <10% RH. The sulfonated COF is characterised extensively and the long-term stability and regeneration of the network is discussed.

Results and discussion

Characterisation of sulfonated covalent organic framework

We synthesised a sulfonated covalent organic framework (COF-SO_3H) via a hydrothermal method following a previous report (Figure 1a).[26,27] In brief, 2,5-diaminobenzenesulfonic acid (DASA), 1,3,5-triformylphloroglucinol (Tp) and p-toluenesulfonic acid (PTSA) were dissolved in water and mixed thoroughly for 20 min using a vortex shaker. The resulting orange mixture was transferred to a Teflon-lined autoclave and heated at 120 °C for 24 h under static conditions, yielding COF-SO_3H as a dark red powder. A more detailed synthesis description can be found in the SI.

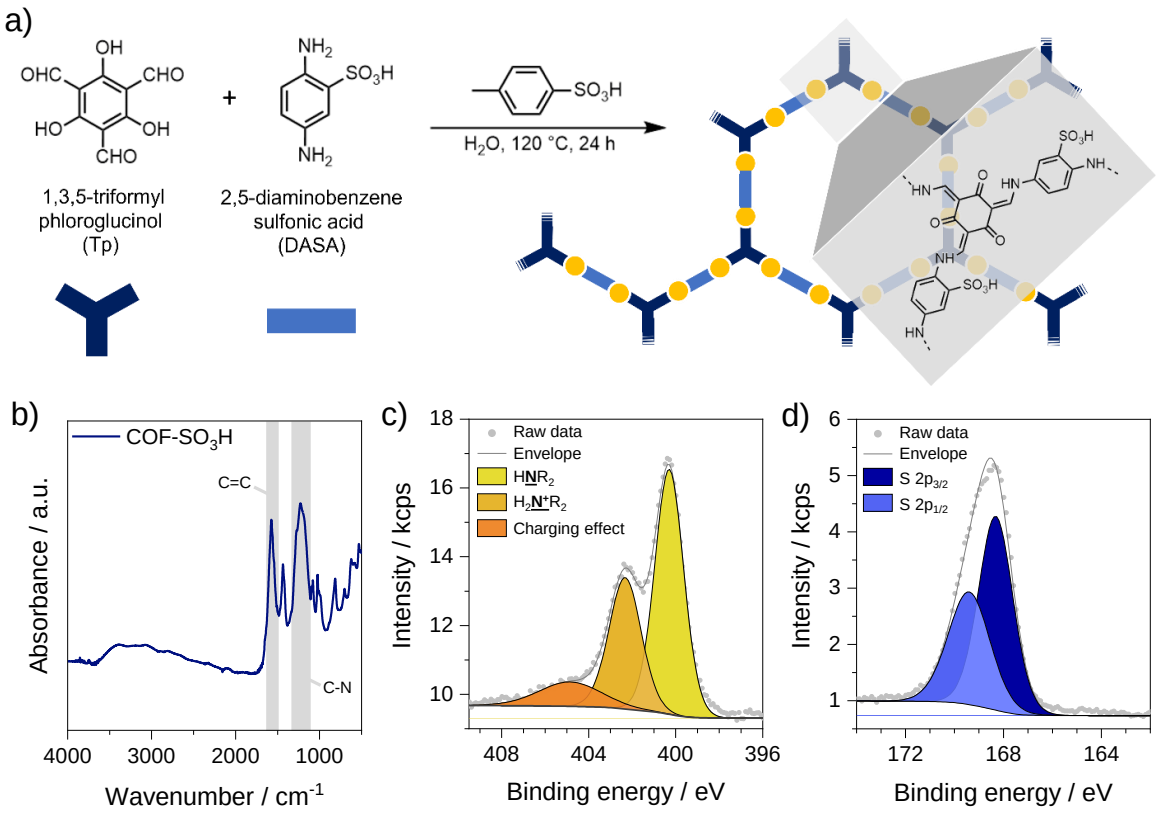

Figure 1. (a) Reaction scheme for the synthesis of COF-SO_3H. (b) FTIR spectrum of COF-SO_3H. (c) X-ray photoelectron N 1s spectrum for COF-SO_3H. (d) X-ray photoelectron S 2p spectrum for COF-SO_3H.

The successful formation of COF-SO_3H was confirmed using Fourier-transform infrared spectroscopy (FTIR). The FTIR spectrum of COF-SO_3H (Figure 1b) confirmed the complete conversion of the starting materials, evidenced by the absence of the characteristic N−H stretching vibrations (3425 and 3335 cm^{-1}) and the −CH=O band (2923 cm^{-1}), corresponding to free diamine in DASA and free aldehyde in Tp, respectively.[28] Furthermore, characteristic signals ascribed to the formation of the β-ketoenamine-linked framework were observed at 1653 cm^{-1} (C=O), 1574 cm^{-1} (C=C), and 1225 cm^{-1} (C−N), respectively. The presence of −SO_3H groups was verified by the appearance of distinctive signals at 1435 cm^{-1}, 1080 cm^{-1}, 1024 cm^{-1}, and 986 cm^{-1}, assigned to S=O and S−OH stretching vibrations.

We performed X-ray photoelectron spectroscopy (XPS) to gain a more in-depth understanding of the chemical composition of COF-SO_3H. The main component of the high-resolution N 1s spectra (Figure 1c), observed at a binding energy of 400.3 eV is attributed to free secondary amine, while signals at 402.3 and 404.8 eV are assigned to protonated secondary amine and charging effects, respectively, confirming the successful condensation reaction between −NH_2

and groups −CHO of DASA and Tp, respectively. The high-resolution S 2p spectrum revealed a typical asymmetric peak for a sulfonic acid moiety (Figure 1d),[29] and the peaks at binding energies of 168.4 eV and 169.4 eV are assigned to S $2p_{3/2}$ and S $2p_{1/2}$, respectively. The surface and bulk chemical composition determined by XPS and elemental analysis, respectively is provided in Table S1, accompanied by a brief discussion of the result.

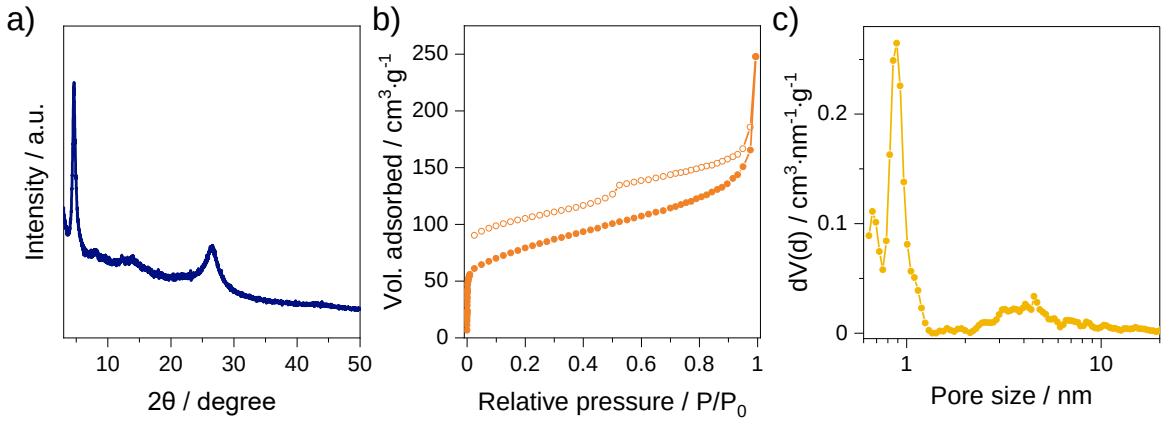

Figure 2. Physical characterisation of COF-SO_3H. a) X-ray diffractogram. b) N_2 isotherm measured at -196 °C (77 K), filled and empty circles represent adsorption and desorption, respectively. c) Pore size distribution obtained by fitting the adsorption branch of the isotherm with the QSDFT kernel.

Powder X-ray diffraction (PXRD) (Figure 2a) revealed the crystalline nature of pristine COF-SO_3H and agrees well with previous reports as well as the simulated spectrum for an eclipsed 2D stacking model structure.[26] Diffraction peaks present at $2\theta = 4.6°$, 8.1° and 26.7°, were attributed to reflection from the (100), (110) and (001) planes, respectively. The broadening of the PXRD peaks can be attributed to a combination of small particle size and small crystalline domains.[28] Thermogravimetric analysis in air confirmed high stability of COF-SO_3H, up to a temperature of ~200 °C (Figure S1). The network exhibits a three-stage weight loss, corresponding to the removal of adsorbed water (50-120 °C), decomposition of sulfonic acid groups (200-370 °C) and the disintegration of the remaining framework (>370 °C). N_2 gas physisorption analysis performed at -196 °C yielded a type I isotherm (Figure 2b), typical for microporous solids. We assume that the gap between adsorption and desorption originates from the swelling behavior of COF-SO_3H. The pronounced porosity manifests in a Brunauer-Emmett-Teller specific surface area (S_{BET}) of 280 m^2 g^{-1} and a total pore volume of

0.23 $cm^3 \cdot g^{-1}$. The pore size distribution of COF-SO_3H was obtained by fitting the adsorption branch of the isotherm with the quenched solid density functional theory (QSDFT) kernel, revealing a predominant pore size of 0.9 nm (Figure 2c). A summary of all of the porous properties of COF-SO_3H is provided in Table S2.

Water sorption experiments

We used dynamic vapour sorption (DVS) to analyse the water-sorption performance of COF-SO_3H and compared it to that of a non-sulfonated equivalent (TpPa-1)[16] to determine the role of the sulfonic acid groups. The water isotherm of COF-SO_3H at 25 °C (Figure 3a) exhibited a steep uptake commencing at <5% RH, corresponding to water condensation in micropores.[30] Previous work showed that TpPa-1 displayed an S-shaped type II isotherm with a steep uptake at ~15% RH.[16] The water uptake in the isotherm of COF-SO_3H is shifted to lower RH, indicating beneficial water-network interactions due to the hydrophilic sulfonate moieties. Upon the integration of sulfonic acid groups into the backbone the total water uptake capacity at 90% RH is slightly reduced from 0.44 $g \cdot g^{-1}$ in TpPa-1[16] to 0.31 $g \cdot g^{-1}$ in COF-SO_3H. This is in good agreement with water sorption isotherms reported for COF-SO_3H in the context of proton conductivity[28] and is likely due to some localised pore collapse upon the evaporation of adsorbed water. We calculated the isosteric heat of adsorption (Q_{st}) to evaluate the strength of water-COF-SO_3H interactions by applying the Clausius−Clapeyron equation to additional isotherms measured at 25 and 35 °C (Figure S2) to be 42 $kJ \cdot mol^{-1}$, which is close to bulk water (Q_{st} = 44 kJ $\cdot mol^{-1}$).[19] Even at 35 and 45 °C, the water sorption isotherm profiles are retained, indicating robust sorption behaviour at higher temperatures. We hypothesise that the sulfonate moieties serve as hydrophilic centres, facilitating the initial bonding of water molecules at low relative humidity, which later promote pore condensation at increased partial pressure.[20]

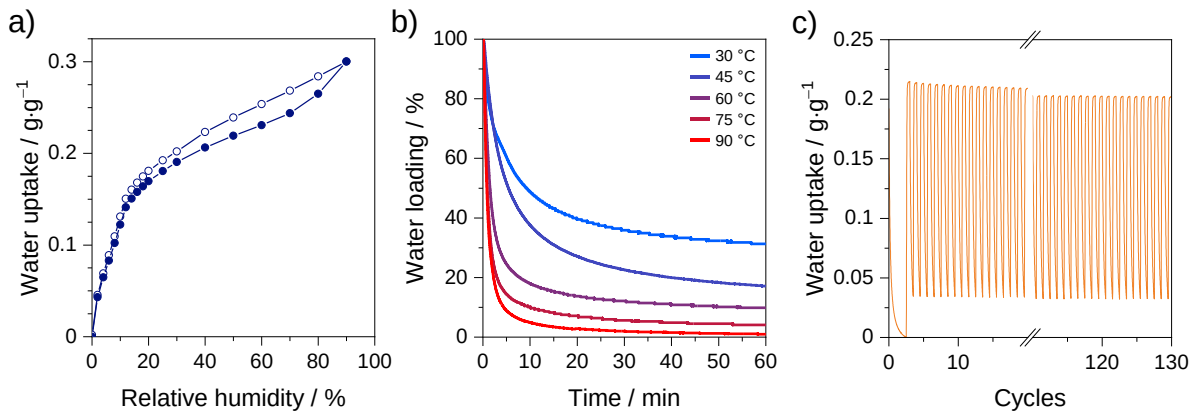

Figure 3. Water sorption-desorption properties of COF-SO_3H. a) H_2O isotherm at 25 °C. Closed spheres represent uptake and open spheres represent desorption. b) Desorption of water over time at various temperatures, measured with TGA. c) Long-term stability of SHCP-10 over 130 adsorption–desorption cycles consisting of a humidity-swing process between 0% and 40% RH.

We exposed dry COF-SO_3H to 10, 20, 30, and 90% RH to investigate the water sorption/desorption behaviour in more detail (Figure S3). Upon exposure to 10% RH, COF-SO_3H adsorbed ~0.13 g·g^{-1} after 24 hours. Notably, 80% of the water adsorption took place within 30 min, and 95% occurred after one hour, demonstrating fast uptake at low RH. Water desorption was triggered by a reversal to 0% RH, and 0.12 g·g^{-1} or 93% of the adsorbed water was removed within 2 h. Comparable adsorption rates were observed at 20%, 30%, and 90% RH, reaching total capacities of 0.17 g·g^{-1}, 0.19 g·g^{-1} and 0.32 g·g^{-1}, respectively.

To demonstrate that water removal could be achieved by heating, COF-SO_3H was first subjected to controlled conditions (~50% RH and 20 °C) for 24 h for water loading and then transferred to a thermogravimetric analyser, where the heat-induced water desorption was monitored for 1 h at temperatures of 30, 45, 60, 75, and 90 °C (Figure 3b). Higher temperatures induced a faster rate of water release and resulted in a more complete removal of the adsorbed water. Water removal rates increased significantly at temperatures above 45 °C, leading to the release of >80% of the absorbed water within 10 min at 60 °C, and >95% over the same time at 90 °C. In conjunction with the rapid uptake rates observed for COF-SO_3H, these findings underline the possibility of performing multiple adsorption-desorption cycles in a single day, substantially enhancing daily water production.

Long-term stability of COF-SO_3H

The stability of adsorbents for AWH is a crucial parameter, as they must maintain their water uptake capacity over multiple adsorption-desorption cycles. We explored the cycling stability of COF-SO_3H by subjecting the network to a total of 130 humidity swings between 0 and 40% RH (Figure 3c, full data available in Figure S4). The initial working capacity of COF-SO_3H was determined to be ~0.21 $g \cdot g^{-1}$ under these conditions and was reduced to ~0.20 $g \cdot g^{-1}$ after 130 adsorption-desorption cycles, equating to a decrease in water uptake of just 4%.

Upon the completion of 130 water sorption-desorption cycles, we re-analysed COF-SO_3H using FTIR, XPS, and PXRD. COF-SO_3H remained unchanged from the pristine material in all cases (Figure S5-S7). Given the onset of water uptake at <5% RH and the apparent stability after 130 adsorption-desorption cycles, COF-SO_3H shows promise for AWH in extreme environments.

Conclusion

We showed a sulfonate-decorated covalent organic framework (COF-SO_3H) capable of low RH atmospheric water harvesting. The network displayed an overall water capacity of up to 0.3 $g \cdot g^{-1}$ at 90% relative humidity (RH) and 25 °C, reaching almost 60% of its total uptake at ≤20% RH. Water uptake began <5% RH, representing a significant improvement in hydrophilicity compared to a non-sulfonated equivalent. Repeated water sorption-desorption cycles showed no significant decrease in uptake performance. In addition to retaining excellent AWH ability, COF-SO_3H showed no measurable chemical change after many water adsorption–desorption cycles. Considering the low RH water uptake of COF-SO_3H, we believe that the design of sulfonated networks could pave the way to high-performance AWH in extreme environments.

Acknowledgement

The authors acknowledge the funding support of the University of Vienna (Austria). The authors thank Mag. Johannes Theiner and the Microanalytical Laboratory (University of Vienna) for their assistance with elemental analysis.

Author contributions

P.S. characterized COF-SO_3H, designed experiments, and performed water sorption/desorption tests. C.L. and P.G. synthesized and characterized COF-SO_3H. F.K. and R.T.W. designed experiments and supervised this work. P.S., P.G., F.K. and R.T.W. wrote and edited the manuscript and all authors discussed the results and commented on the manuscript.

Competing Interests

There are no conflicts of interest to declare.

Author Information

Corresponding Authors

Univ.-Prof. Dr. Freddy Kleitz - Department of Functional Materials and Catalysis, Faculty of Chemistry, University of Vienna, 1090 Vienna, Austria; ORCID: 0000-0001-6769-4180. E-mail: freddy.kleitz@univie.ac.at.

Ass.-Prof. Dr. Robert T. Woodward - Institute of Materials Chemistry and Research, Faculty of Chemistry, University of Vienna, 1090, Vienna, Austria; ORCID: 0000-0003-0834-5137. E-mail: robert.woodward@univie.ac.at.

Authors

Paul Schweng - Institute of Materials Chemistry and Research, Faculty of Chemistry, University of Vienna, 1090, Vienna, Austria; ORCID: 0009-0008-4218-377X. E-mail: paul.schweng@univie.ac.at.

Dr. Changxia Li - Department of Functional Materials and Catalysis, Faculty of Chemistry, University of Vienna, 1090 Vienna, Austria; ORCID: 0000-0001-8266-3649. E-mail: changxia.li@univie.ac.at.

Patrick Guggenberger - Department of Functional Materials and Catalysis, Faculty of Chemistry, University of Vienna, 1090 Vienna, Austria; ORCID: 0000-0002-2521-6997. E-mail: patrick.guggenberger@univie.ac.at.

References

[1] United Nations, The Sustainable Development Goals Report 2022. https://unstats.un.org/sdgs/report/2022/ (accessed 2023-08-18).
[2] M. Elimelech, W. A. Philip, *Science* **2011**, *333* (6043), 712-717. DOI: 10.1126/science.1200488
[3] H. Nassrullah, S. F. Anis, R. Hashaikeh, N. Hilal, *Desalination* **2020**, *491*, 114569. DOI: 10.1016/j.desal.2020.114569
[4] W. Shi, W. Guan, C. Lei, G. Yu, *Angew. Chemie. Int. Ed.* **2022**, 61, e202211267. DOI: 10.1002/anie.202211267
[5] P. Gleick, in *Water in Crisis: A Guide to the World's Fresh Water Resources*, Oxford University Press, Oxford 1993, pp. 13–24.
[6] L. Zhang, W.-X. Fang, C. Wang, H. Dong, S.-H. Ma, Y.-H. Luo., *Inorg. Chem. Front.* **2021**, *8*, 898-913. DOI: 10.1039/d0qi01362e
[7] H. W. B. Teo, A. Chakraborty, W. Fan, *Microporous Mesoporous Mater.* **2017**, *242*, 109–117. DOI: 10.1016/j.micromeso.2017.01.015
[8] R. Li, Y. Shi, L. Shi, M. Alsaedi, P. Wang, *Environ. Sci. Technol.* **2018**, *52* (9), 5398–5406. DOI: 10.1021/acs.est.7b06373
[9] M. Kalmutzki, C. S. Diercks, O. M. Yaghi, *Adv. Mater.* **2018**, *30* (37), 1704304. DOI: 10.1002/adma.201704304
[10] W. Song, Z. Zheng, A. H. Alawadhi, O. M. Yaghi, *Nat. Water.* **2023**, *1*, 626-634. DOI: 10.1038/s44221-023-00103-7
[11] X. Liu, X. Wang, F. Kapteijn, *Chem. Rev.* **2020**, *120* (16), 8303-8377. DOI: 10.1021/acs.chemrev.9b00746
[12] H. L. Nguyen, *Adv. Mater.* **2023**, *35* (17), 2300018. DOI: 10.1002/adma.202300018
[13] M. S. Lohse, T. Bein, *Adv. Funct. Mater.* **2018**, *28* (33), 1705553. DOI: 10.1002/adfm.201705553
[14] N. Huang, P. Wang, D. Jiang, *Nat. Rev. Mater.* **2016**, *1*, 16068. DOI: 10.1038/natrevmats.2016.68
[15] L. Grunenberg, G. Savasci, S. T. Emmerling, F. Heck, S. Bette, A. C. Bergesch, C. Ochsenfeld, B. V. Lotsch, *J. Am. Chem. Soc.* **2023**, *145* (24), 13241–13248. DOI: 10.1021/jacs.3c02572
[16] B. P. Biswal, S. Kandambeth, S. Chandra, D. B. Shinde, S. Bera, S. Karak, B. Garai, U. K. Kharul, R. Banerjee, *J. Mater. Chem. A.* **2015**, *47* (3), 23664-23669. DOI: 10.1039/C5TA07998E
[17] L. Stegbauer, M. W. Hahn, A. Jentys, G. Savasci, C. Ochsenfeld, J. A. Lercher, B. V. Lotsch, *Chem. Mater.* **2015**, *27* (23), 7874–7881. DOI: 10.1021/acs.chemmater.5b02151
[18] F. Wen, X. Wu, X. Li, N. Huang, *Chem. Eur. J.* **2023**, *just accepted*. DOI: 10.1002/chem.202302399
[19] H. L. Nguyen, N. Hanikel, S. J. Lyle, C. Zhu, D. M. Proserpio, O. M. Yaghi, *J. Am. Chem. Soc.* **2020**, *142* (5), 2218–2221. DOI: 10.1021/jacs.9b13094
[20] K. T. Tan, S. Tao, N. Huang, D. Jiang, *Nat. Commun*. **2021**, *12*, 6747. DOI: 10.1038/s41467-021-27128-4
[21] H. L. Nguyen, C. Gropp, N. Hanikel, A. Möckel, A. Lund, O. M. Yaghi, *ACS Cent. Sci.* **2022**, *8* (7), 926–932. DOI: 10.1021/acscentsci.2c00398

[22] L.-H. Chen, W.-K. Han, X. Yan, J. Zhang, Y. Jiang, Z. G. Gu, *ChemSusChem* **2022**, *15* (24), e202201824. DOI: 10.1002/cssc.202201824
[23] C. Sun, Y. Zhu, P. Shao, L. Chen, X. Huang, S. Zhao, D. Ma, X. Jing, B. Wang, X. Feng, *Angew. Chem. Int. Ed.* **2023**, *62* (11), e202217103. DOI: 10.1002/anie.202217103
[24] Q. Zhu, X. Wang, R. Clowes, P. Cui, L. Chen, M. A. Little, A. I. Cooper, *J. Am. Chem. Soc.* **2020**, *142* (39), 16842–16848. DOI: 10.1021/jacs.0c07732
[25] P. Schweng, F. Mayer, D. Galehdari, K. Weiland, R. T. Woodward, *Small* **2023**, 2304562. DOI: 10.1002/smll.202304562
[26] C. Li, S. Cao, J. Lutzki, J. Yang, T. Konegger, F. Kleitz, A. Thomas, *J. Am. Chem. Soc.* **2022**, *144* (7), 3083–3090. DOI: 10.1021/jacs.1c11689
[27] C. Li, P. Guggenberger, S. W. Han, W.-L. Ding, F. Kleitz, *Angew. Chem. Int. Ed.* **2022**, *61* (35), e202206564. DOI: 10.1002/anie.202206564
[28] S. Chandra, T. Kundu, K. Dey, M Addicoat, T. Heine, R. Banerjee, *Chem. Mater.* **2016**, *28* (5), 1489–1494. DOI: 10.1021/acs.chemmater.5b04947
[29] A. Blocher, F. Mayer, P. Schweng, T. M. Tikovits, N. Yousefi, R. T. Woodward, *Mater. Adv.* **2022**, *3* (15), 6335–6342. DOI: 10.1039/D2MA00379A
[30] N. Hanikel, X. Pei, S. Chheda, H. Lyu, W. Jeong, J. Sauer, L. Gagliardi, O. M. Yaghi, *Science* **2021**, *374* (6566), 454−459. DOI: 10.1126/science.abj0890